2001-01-0503

SIMON: A New Vehicle Simulation Model for Vehicle Design and Safety Research

Terry D. Day
Sydney G. Roberts
Engineering Dynamics Corporation

Allen R. York
A. R. York Engineering

ABSTRACT

SIMON is a new vehicle dynamic simulation model. Applications for SIMON include single- and multi-unit vehicle handling simulation in severe limit maneuvers (including rollovers) and 3-dimensional environments. Applications also include vehicle-to-vehicle and vehicle-to-barrier collisions. This paper provides the technical background for the SIMON engineering model. The 3-dimensional equations of motion used by the model are presented and explained in detail. The calculations for suspension, tire, collision, aerodynamic and inter-vehicle connection forces and moments are also developed. The integration of features available in the HVE Simulation Environment, such as DyMESH, the Driver Model, Brake Designer and Steer Degree of Freedom, is also explained. Finally, assumptions and limitations of the model are presented.

VEHICLE SIMULATION has many uses in the vehicle design and safety industries. Applications include vehicle design (suspension modeling, vehicle-tire system modeling and brake system modeling), virtual prototyping and compliance testing (ISO braking and lane change maneuvers) and safety analysis (collision simulation and post-crash reconstruction of actual events).

Advances in vehicle modeling and computer hardware and software technology have made possible significant improvements in the field of vehicle simulation, resulting in newer and more powerful modeling capability. For example, simulations in the 1980's typically used 2-dimensional models employing three degrees of freedom. More sophisticated models existed, but were not often used because of their crude user interfaces.

In 1996, the HVE simulation environment was introduced [1-6]*. HVE (Human-Vehicle-Environment) was developed as a sophisticated, 3-dimensional user environment for executing simulations involving humans and vehicles. HVE was designed to be a general purpose tool, making few assumptions about the details of the actual simulation. These details were left up to the designer/programmer of the simulation model.

Several HVE-compatible simulation models were developed at the time of HVE's introduction. These models included passenger car simulations (e.g., EDVSM [7,8]), commercial vehicle simulations (e.g., EDVDS [9,10]) and human occupant simulations (e.g., EDHIS [11]). Collision simulation models were also made available (e.g., EDSMAC4 [12,13]). However, none of these individual models included all the features required by the vehicle design and safety industries.

A new model, named SIMON (**SI**mulation **MO**del **N**on-linear [14]), has been developed that encompasses all the individual features in the above models. In addition, SIMON is the first model to take full advantage of the capabilities found in the HVE simulation environment.

This paper presents a detailed overview of the SIMON model.

---

*Numbers in brackets designate references found at the end of the paper.

OVERVIEW

SIMON is a dynamic simulation model of the response of one or more vehicles to driver inputs, inter-vehicle collision(s) and factors related to the environment (e.g., terrain, atmosphere). SIMON is a newly developed simulation model, using a new, general purpose 3-dimensional vehicle dynamics engine. The dynamics engine allows a sprung mass with six degrees of freedom and multiple axles with up to five degrees of freedom per axle. SIMON was specifically designed to take advantage of the rich feature set available in the HVE simulation environment, including the HVE Brake Designer [6,15], Driver Model [6,16] and Tire Blow-out Model [6,17].

General Features and Capabilities

Each SIMON vehicle may have up to three axles (six axles for full trailers) and single or dual tires. Independent and solid axle suspensions are allowed. SIMON may be used for numerous types of simulation studies. Applications for SIMON include:

- **Single Vehicle Simulation -** SIMON's 3-dimensional vehicle dynamics model incorporates robust tire and suspension models required for vehicle handling simulation studies, including rollover.
- **Articulated Vehicle Simulation -** SIMON's vehicle dynamics model also simulates articulated, multi-vehicle trains. The model is general and allows the user to model numerous vehicle/trailer configurations.
- **Collision Simulation -** SIMON incorporates DyMESH [18,19], a patented, general-purpose, 3-dimensional collision model for simulating vehicle-to-vehicle and vehicle-to-barrier collisions.
- **Vehicle Design -** SIMON may be used for vehicle design projects involving suspension, brake, tire and steering systems. Using SIMON, these systems may be optimized on the computer before expensive prototyping and testing begins. Parametric studies involving in-use factors (such as weight distribution changes due to occupant loading and payload location) may also be performed.
- **Safety Research -** Safety researchers may use SIMON for reconstructing most crashes involving single or multiple vehicles. Human, vehicle and environment factors may be simulated and evaluated to assist in performing detailed crash studies. Crashes involving multiple vehicles and irregular terrain are also handled.

Model Inputs

SIMON inputs include one or more vehicles. Articulated vehicles are created from individual unit vehicles using compatible front and rear connections. Full trailers are created using a semi-trailer and a front dolly.

For collision simulation, a 3-D geometry file (or *body mesh*) is required. The DyMESH impact model uses the body mesh vertex 3-D coordinates and supplemental information (e.g., friction, force-deflection properties) as inputs to the model.

Human occupants may also be included in SIMON. Placing a human in a vehicle affects the vehicle's inertial properties and weight distribution. However, human motion relative to the vehicle is not modeled.

An environment geometry file is optional. If supplied, the complexity of the environment may range from a simple flat surface to a complex 3-D digital terrain map (DTM) from a total station survey of a vehicle manufacturer's proving ground facility [19]. Interaction between the tire and terrain at various terrain locations is modeled by assigning different parameters (e.g., friction multiplier) to different regions of the DTM. These are referred to as *friction zones*; an unlimited number of friction zones may be included. Terrain elevation and surface normals (i.e., slopes) for each location in the environment are interpreted directly from the DTM geometry.

Model Outputs

The output from a SIMON simulation is displayed in the following HVE Output Reports:

- **Accident History -** A report displaying vehicle positions and velocities at *Initial, Impact, Separation* and *Final/Rest* positions
- **Damage Profiles (for collision simulation) -** A 3-dimensional visual simulation of the vehicle deformation as it progresses during the collision
- **Driver Controls -** A report displaying driver inputs (*Steering, Braking, Throttle,* and *Gear Selection*) for each vehicle
- **Environment Data -** A report displaying the basic information describing the crash environment (e.g., *Barometric Pressure, Temperature, Gravity Constant*)
- **Event Data -** A report of event-related factors (*Tire Blow-out, Wheel Displacement* and *Initial Brake* parameters) and *Accelerometer Locations* for each vehicle
- **Human Data -** A report of weights and seat position coordinates for each vehicle occupant
- **Messages -** A list of diagnostics produced for the event
- **Program Data -** Basic SIMON version information
- **Trajectory Simulation -** A 3-dimensional visual simulation of the vehicle motion
- **Variable Output -** A table of user-selected, time-dependent simulation outputs for each vehicle
- **Vehicle Data -** A report displaying the vehicle properties for each vehicle in the event

Validation

The initial validation of SIMON is under way and is not yet complete. The suite of validations includes comparison with well instrumented full-scale experiments that include limit handling maneuvers, collisions between unit and articulated vehicles, and rollovers. This test matrix represents a cross-section of the types of events for which SIMON was intended. It is anticipated that additional validations will be published as they are performed.

MATHEMATICAL MODEL

SIMON is a dynamic simulation analysis of one or more vehicles. SIMON is a new simulation model, incorporating a new, general purpose 3-dimensional dynamics engine. The SIMON model includes a sprung mass with six degrees of freedom (*x,y,z,roll,pitch,yaw*) and unsprung masses with three degrees of freedom per axle (axle *roll*, *z* and *steer* for solid axle suspensions; axle *steer* and right and left wheel *z* for independent suspensions). Wheel *spin* is also included for each wheel location.

The vehicle model includes the following basic components for each vehicle unit:

- Sprung mass inertial properties
- Up to three axles (full trailers may have up to six axles)
- Independent or solid axle suspension for each axle
- Single or dual tires at each wheel location
- Front and rear inter-vehicle connections
- Exterior body geometry
- Aerodynamic surface(s)
- Payload(s)
- Human occupant(s)
- Steering system
- Braking system
- Drivetrain (engine, transmission, differential)

The basic vehicle model is shown in Figure 1.

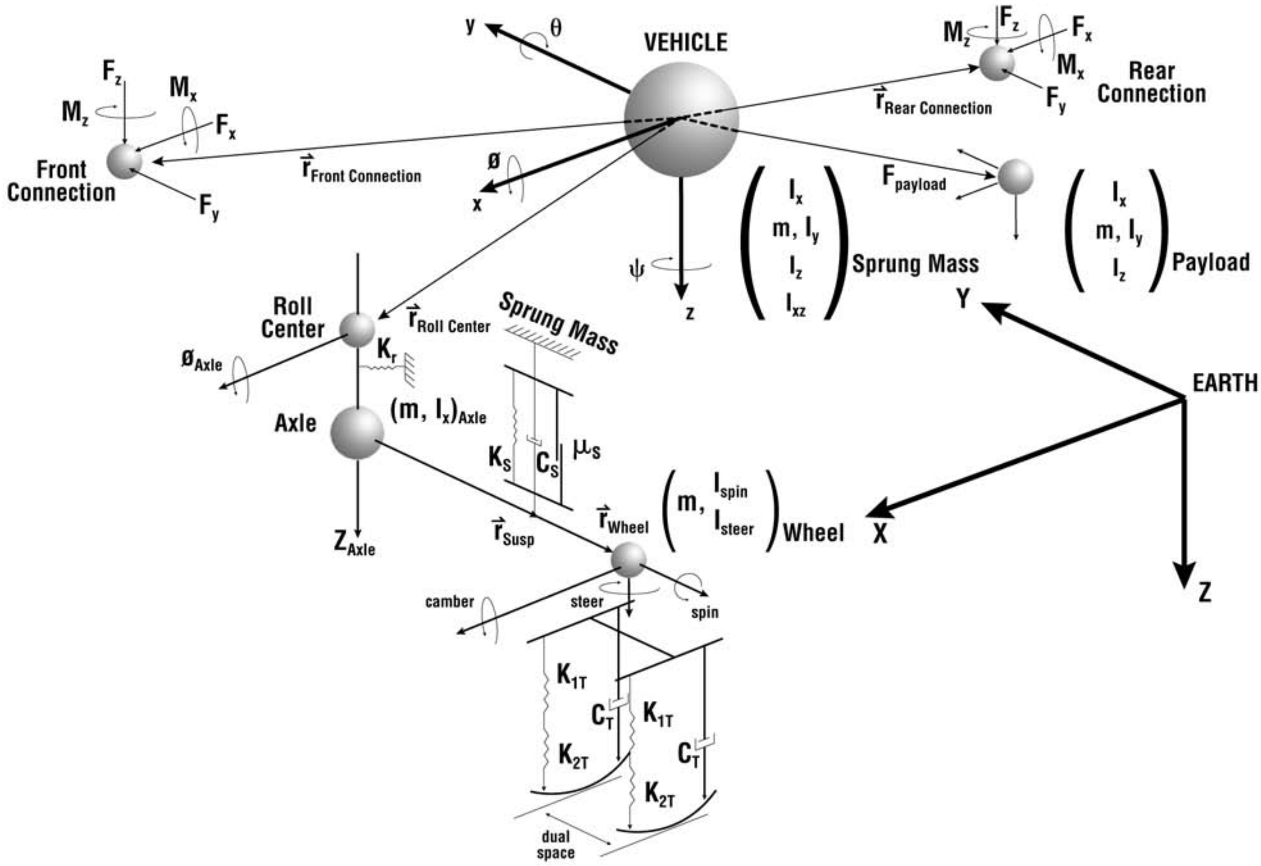

Figure 1 - SIMON mathematical model.

Equations of Motion

The system of equations requires three coordinate systems:

- **Inertial reference system –** This is the earth-fixed coordinate system defined by a right-handed, orthogonal X,Y,Z coordinate axis system. The Z-axis is parallel to the gravity vector, hence it is pointed downward. The X and Y directions and the location of the origin are arbitrary (within the requirement of orthogonality).
- **Vehicle reference system –** This is the vehicle-fixed coordinate system defined by a right-handed, orthogonal x,y,z coordinate system attached to the sprung mass. Its origin is coincident with the sprung mass center of gravity (CG). The x-axis defines the forward vehicle direction, the y-axis points to the vehicle's right side and the z-axis points towards the bottom of the vehicle.
- **Tire reference system –** This is the tire-fixed coordinate system defined by a right-handed, orthogonal coordinate system fixed to the tire. Its origin is the perpendicular intersection between the tire plane, the road plane (i.e., terrain) and a plane through the wheel center. The x'-axis lies in the road plane and points in the tire-fixed forward direction, the y'-axis points to the right and the z'-axis is a radial vector in the tire plane normal to the road plane.

These coordinate systems follow SAE Recommended Practice J-670e [21].

The equations that govern the general, non-linear, unsteady motion of the vehicle sprung mass are based on Euler's equations of motion written with respect to the (moving) vehicle reference system. The choice of the moving reference frame greatly simplifies the calculation of external forces and avoids the appearance of the moments and products of inertia in the equations of motion. The derivation for these equations may be found in reference 22. A more detailed version of the following development may also be found in reference 14, chapter 4.

The equations of motion take the general form

$$
\begin{aligned}
\sum F_x &= m\left(\dot{u} + wq - vr\right) \\
\sum F_y &= m\left(\dot{v} + ur - wp\right) \\
\sum F_z &= m\left(\dot{w} + vp - uq\right) \\
\sum M_x &= \dot{L}_x + qL_z - rL_y \\
\sum M_y &= \dot{L}_y + rL_x - pL_z \\
\sum M_z &= \dot{L}_z + pL_y - qL_x
\end{aligned} \qquad \text{(Eqs. 1)}
$$

where

u,v,w	=	Vehicle-fixed components of linear velocity
p,q,r	=	Vehicle-fixed components of angular velocity
F_x,F_y,F_z	=	Vehicle-fixed components of external forces
M_x,M_y,M_z	=	Vehicle-fixed components of external moments
L_x,L_y,L_z	=	Vehicle-fixed components of angular momentum

Assuming symmetry in the x-y and y-z planes, the x-y and y-z products of inertia are zero. However, symmetry is not assumed in the x-z plane, so I_{xz} is included in the angular equations. Thus,

$$
\begin{aligned}
M_x &= I_x\dot{p} - I_{xz}\dot{r} - qr\left(I_y - I_z\right) - qpI_{xz} \\
M_y &= I_y\dot{q} - \left(r^2 - p^2\right)I_{xz} - rp\left(I_z - I_x\right) \\
M_z &= I_z\dot{r} - I_{xz}\dot{p} - pq\left(I_x - I_{xy}\right) + qrI_{xz}
\end{aligned} \qquad \text{(Eq. 2)}
$$

Sprung Mass

In the derivation that follows, the Euler equations of motion include the inertial coupling effects of the unsprung masses. When combined with the other applied external forces acting on the sprung mass,

$$
\sum \vec{F}_{Total} = \sum \vec{F}_{Suspension} + \sum \vec{F}_{Connection} + \sum \vec{F}_{Collision} + \sum \vec{F}_{Aerodynamic} + \sum \vec{F}_{Unsprung\,Mass} \qquad \text{(Eq. 3)}
$$

where

$\sum \vec{F}_{Suspension}$	=	Sum of vehicle-fixed components of suspension forces
$\sum \vec{F}_{Connection}$	=	Sum of vehicle-fixed components of connection forces
$\sum \vec{F}_{Collision}$	=	Sum of vehicle-fixed components of collision forces

(forces on sprung mass, continued):

$\sum \vec{F}_{Aerodynamic}$ = Sum of vehicle-fixed components of aerodynamic forces

$\sum \vec{F}_{Unsprung\,Mass}$ = Sum of vehicle-fixed components of inertial forces from unsprung masses (described in the next section)

Unsprung Mass

Calculation of the motion of the sprung mass requires the contributions of the inertial coupling of the unsprung masses in the vehicle-fixed x- and y-directions. Thus, the calculation of the vehicle-fixed components of acceleration of the unsprung masses is necessary. Assuming the unsprung masses are point masses moving with respect to the (moving) vehicle, the vehicle-fixed accelerations for an unsprung mass are

$$a_x = \dot{u} - vr + wq + \ddot{x} + 2q\dot{z} - 2r\dot{y} - x\left(q^2 + r^2\right) + y\left(pq - \dot{r}\right) + z\left(pr + \dot{q}\right) \quad \text{(Eq. 4)}$$

$$a_y = \dot{v} + ur - wp + \ddot{y} + 2r\dot{x} - 2p\dot{z} + x\left(pq + \dot{r}\right) + y\left(p^2 + r^2\right) + z\left(qr - \dot{p}\right) \quad \text{(Eq. 5)}$$

where

x,y,z = vehicle-fixed components for location of unsprung mass CG's

The acceleration in the z-direction is not required because the unsprung masses are not directly coupled in the z-direction.

The constraints placed on the motion of the unsprung masses by the connections between the sprung and unsprung masses are such that there is no relative motion between the unsprung and sprung masses in the vehicle-fixed x-direction. Thus, $\ddot{x}$=0. Therefore, in Newton's 2nd law form, the inertial coupling forces for unsprung mass i may be rewritten as

$$F_{x_i} = m_i a_{x_i} = m_i \begin{pmatrix} \dot{u} - vr + wq + 2q\dot{z}_i + 2r\dot{y}_i - x_i\left(q^2 + r^2\right) + \\ y_i\left(pq + \dot{r}\right) + z_i\left(pr + \dot{q}\right) \end{pmatrix} \quad \text{(Eq. 6)}$$

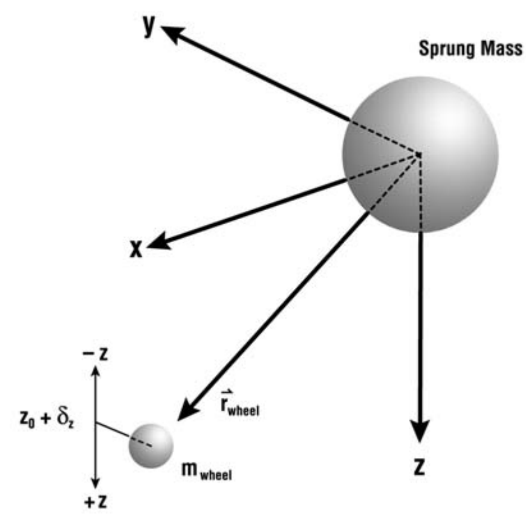

Figure 2 - Degrees of freedom for an independent suspension. Dynamic motion of each wheel is defined in the vehicle-fixed z-direction (spin and steer angular dynamic motion may also be defined as an option; see Wheel Spin and Steering System sections).

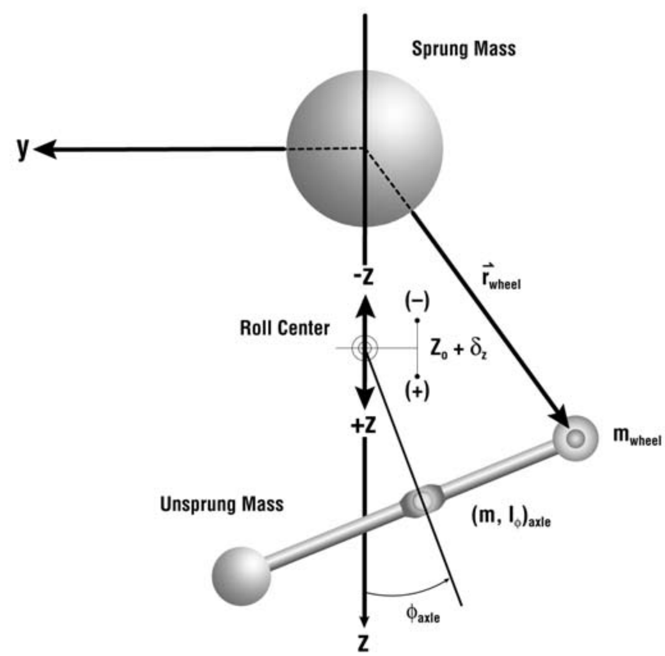

Figure 3 - Degrees of freedom for a solid axle suspension. Dynamic motion of each axle is defined in the vehicle-fixed z-direction and ϕ rotation (spin and steer angular dynamic motion may also be defined as an option; see Wheel Spin and Steering System sections).

and

$$F_{y_i} = m_i a_{y_i} = m_i \begin{pmatrix} \dot{v} + ur - wp - 2p\dot{z}_i + x_i\left(pq + \dot{r}\right) - \\ y_i\left(p^2 + r^2\right) + z_i\left(qr - \dot{p}\right) \end{pmatrix}$$

(Eq. 7)

The unsprung mass *x,y,z* positions and their derivatives appear in the above inertial coupling equations. Thus, the vehicle-fixed positions, velocities and accelerations for the unsprung masses are required. These kinematics are different for independent and solid axle suspension types. These details may be found in Reference 14.

Wheel Spin

Calculation of the wheel spin velocity, Ω, requires the wheel spin acceleration, $\dot{\Omega}$. Spin acceleration arises from drive and brake torques and from tire rolling resistance, as shown in the free-body diagram in Figure 4 (for purposes of clarification, only torque-producing forces are shown in the figure).

For driven axles, the model is complicated by the introduction of the coupling effect of the differential and from the introduction of drivetrain rotational inertia. The differential equation for the spin degree of freedom at each wheel includes these effects,

$$\left(I_{Wheel,Rt} + \frac{I_{Drivetrain}\eta_{Diff}^2}{4}\right)\frac{d}{dt}\Omega_{Wheel,Rt} + \left(\frac{I_{Drivetrain}\eta_{Diff}^2}{4}\right)\frac{d}{dt}\Omega_{Wheel,Lt} = \left[F_{x'}r + M_{Rolling} + T_b + \eta_{Diff}\left(\zeta T_d\right)\right]_{Right\ Tires}$$

(Eq. 8)

$$\left(I_{Wheel,Lt} + \frac{I_{Drivetrain}\eta_{Diff}^2}{4}\right)\frac{d}{dt}\Omega_{Wheel.Lt} + \left(\frac{I_{Drivetrain}\eta_{Diff}^2}{4}\right)\frac{d}{dt}\Omega_{Wheel,Rt} = \left[F_{x'}r + M_{Rolling} + T_b + \eta_{Diff}\left(\zeta T_d\right)\right]_{Left\ Tires}$$

(Eq. 9)

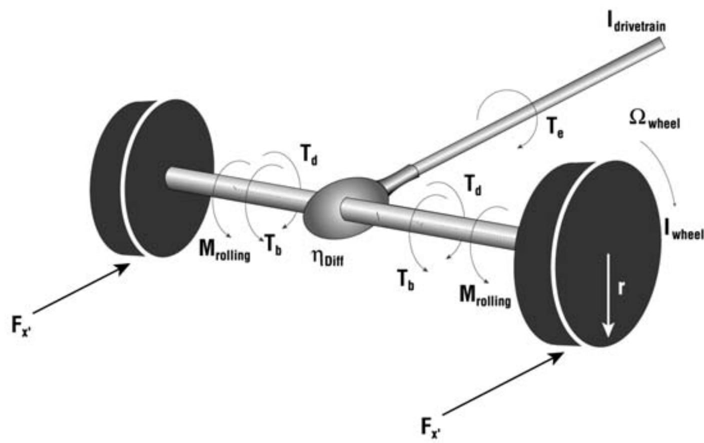

Figure 4 - Wheel spin degree of freedom moments and forces.

The solution of Eqs. 8 and 9 for wheel spin acceleration, $\dot{\Omega}$, yields

$$\dot{\Omega}_{Wheel,Rt} = \zeta_{Wheel,Rt}\left(T_d \times \eta_{Diff} + T_b - F_{x'}r + M_{Rolling}\right)_{Wheel,Rt} - \zeta_{Wheel,Lt}\left(T_d \times \eta_{Diff} + T_b - F_{x'}r + M_{Rolling}\right)_{Wheel,Lt}$$

(Eq. 10)

and

$$\dot{\Omega}_{Wheel,Lt} = \zeta_{Wheel,Rt}\left(T_d \times \eta_{Diff} + T_b - F_{x'}r + M_{Rolling}\right)_{Wheel,Lt} - \zeta_{Wheel,Lt}\left(T_d \times \eta_{Diff} + T_b - F_{x'}r + M_{Rolling}\right)_{Wheel,Rt}$$

(Eq. 11)

Once $\dot{\Omega}$ is determined for each wheel, the wheel spin velocity is integrated directly,

$$\Omega = \Omega_{Prev} + \int \dot{\Omega}dt \qquad \text{(Eq. 12)}$$

In the preceding development,

Ω = Wheel spin velocity

Ω_{Prev} = Wheel spin velocity during previous integration timestep

T_d = Wheel drive torque
$= T_e \times \eta_{Trans} \times \eta_{Diff} \times \zeta$ (Eq. 13)

T_e = Engine torque

η_{Trans} = Transmission ratio

η_{Diff} = Differential ratio

ζ = *Torque Function* (fraction of engine torque applied to specified wheel)

$F_{x'}$ = Tire circumferential force

r = Tire effective rolling radius

M = Tire rolling resistance moment

I_{Wheel} = Total wheel spin inertia: tire + rim (×2 if dual tires) + axle + any spinning portion of brake

$I_{Drivetrain}$ = Total rotational inertia of drivetrain components: engine + transmission + driveline

ξ = Wheel inertial factor

$= \dfrac{B}{B-A}$ for the right-side wheel

$= \dfrac{A}{C-A}$ for the left-side wheel

where

$$A = \frac{I_{Drivetrain}\,\eta_{Diff}^2}{4}$$

$$B = I_{Wheel,\,Rt} + A$$

$$C = I_{Wheel,\,Lt} + A$$

In the calculation of wheel drive torque, T_d (above), ζ is the *torque function* that determines how the drive torque is distributed between the drive wheels. By default, SIMON assumes the drive torque is split equally between all drive wheels.

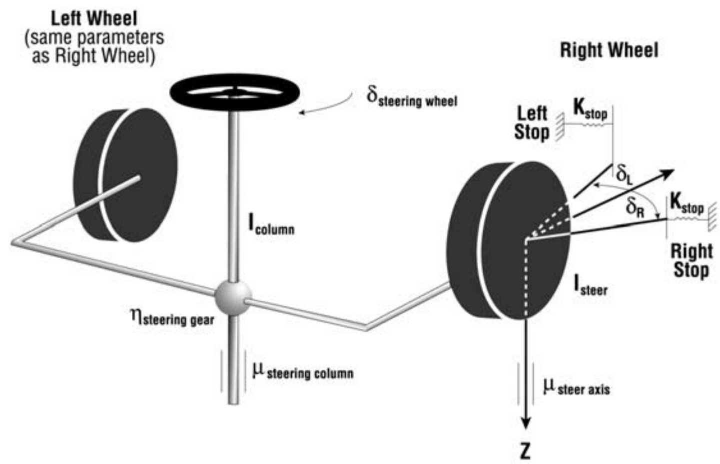

Figure 5 - Steering system model used for Steer Degree of Freedom option.

Steering System

The steering system includes the steering gear ratio (steer angle at the steering wheel divided by the steer angle at the axle). This ratio is used when the *At Steering Wheel* steer table option is selected. Ackerman steering is not supported directly, but may be approximated using the *At Axle* steer table option.

SIMON also incorporates a Steer Degree of Freedom model. The engineering model used by the Steer Degree of Freedom option is shown in Figure 5. The linkage is assumed to be rigid, thus the angular acceleration about the steering axis is the same for right-side and left-side wheels. External tire forces generated at the tire-road interface produce moments at each steerable wheel about the steering axis according to the tire pneumatic trail. The moments are resisted by steer system inertia and internal coulomb friction. Steering is limited by right and left steering stops at each wheel.

Application of Newton's 2nd law to the steering system, ignoring inertial coupling effects, results in

$$\sum M_{Steering} = I_{Steering}\,\ddot{\psi} \qquad \text{(Eq. 14)}$$

where

$\sum M_{Steering}$ = Sum of external moments acting on steering system components

$I_{Steering}$ = Total rotational inertia of steering system components

ψ = Steer angle of each steerable wheel about its steering axis (thus, ψ is the angular acceleration)

The sum of external moments on the entire steering system is

$$\sum M_{Steering} = M_{Stops} + M_{Steer\,Axis\,Friction} + M_{Steering\,Column\,Friction} + M_{Tires} \qquad \text{(Eq. 15)}$$

where

M_{Stops} = Moments about wheel steer axis produced by contact with steering stops

$M_{Steer\,Axis\,Friction}$ = Moments about wheel steer axis produced by coulomb friction in the steering ball joints or king pin

$M_{Steering\,Column\,Friction}$ = Moment about the steering column axis produced by coulomb friction between the steering shaft and bushings or bearings

M_{Tires} = Moments about the wheel steer axis produced by the tire forces and pneumatic trail at the tire-ground shear interface (contact patch)

Steering Stop Torque

Steer angles are limited by elastic steering stops at the right- and left-side wheels, as shown in Figure 6. Each wheel's steering stops limit the steer angle for both right and left steering inputs; the right-steer and left-steer stop angles and mechanical properties need not be equal.

For example, it is possible during a left turn for the stop at the left-side wheel to engage before the stop for the right-side wheel. Steering stop torques can become significant during post-crash yaw. Experiments show that the wheels return to near-zero steer angle fairly quickly, however.

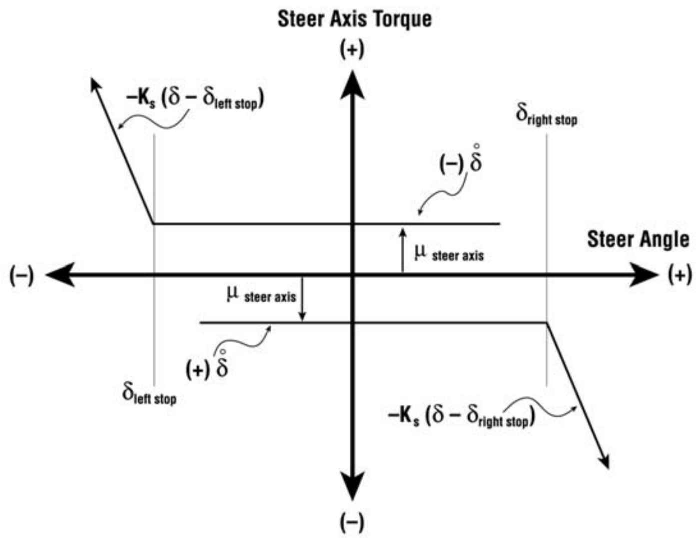

Figure 6 - Steer axis friction and stop torque vs. steer angle.

Steer Axis Torque

Torque is also produced by steering rotation of the wheel about its steer axis. However, no torque is produced unless the steer velocity is non-zero. Thus, a minimum value of steer velocity is required to develop the assigned frictional torque, as shown in Figure 6. This minimum steer velocity is defined by the *friction null band*.

Steering Column Torque

The steering column and steering gear introduce additional friction torque. Like steer axis torque, described above, there is no steering column frictional torque unless the steer velocity is non-zero.

Tire-Ground Torque

Forces at the tire-ground shear interface are the external input to the steering system. Because these forces do not act through the steer axis at its intersection with the ground plane (see Figure 7), an external moment is produced.

Payloads

SIMON supports a payload on each unit vehicle. Note that this means the tow vehicle, trailer(s) and dolly(s) may each have individual payloads. The effect of the payload(s) is simply to change the CG location and inertial properties of the vehicle's sprung mass.

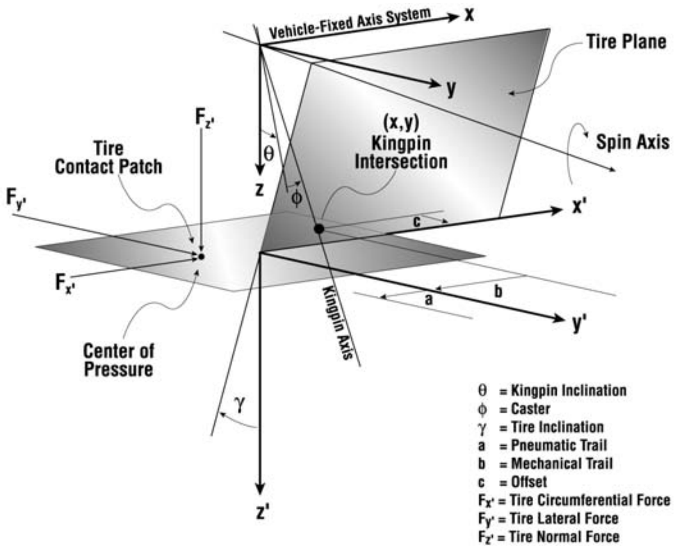

Figure 7 - Close-up view of torque-producing mechanism at tire-ground shear interface.

Given a payload with inertial properties m, I_x, I_y, I_z, placing the payload at a distance, $\vec{r}$, from the sprung mass center of gravity changes the sprung mass center of gravity location as follows:

$$m_{Total} = m_{Sprung} + m_{Payload} \qquad \text{(Eq. 16)}$$

$$\eta = \frac{m_{Payload}}{m_{Total}} \qquad \text{(Eq. 17)}$$

$$\Delta_x = \eta r_x$$

$$\Delta_y = \eta r_y \qquad \text{(Eq. 18)}$$

$$\Delta_z = \eta r_z$$

where

$\vec{\Delta}$ = Change in CG location due to payload

Static wheel loads are modified accordingly. In addition, the parallel axis theorem is used to modify the sprung mass rotational inertias.

Human Occupants

Human occupants may be added to vehicles. Mathematically, the result is equivalent to adding multiple payloads, using the procedures described above. The effect is to change the inertial properties and weight distribution of the vehicle. Humans do not move relative to the vehicle; their motion is not simulated. However, the effect of the occupants on vehicle inertia and handling can be significant.

Driver Controls

SIMON supports user-entered driver controls for steering, braking, throttle and gear selection. These driver controls are entered in the form of open-loop tables of driver input vs. time.

Steering

Steering inputs may be provided for right and left side wheels at each steerable axle. *At Steering Wheel* and *At Axle* options are supported. If the *At Steering Wheel* option is selected, the right side and left side wheel steer angles are equal to the current table entry divided by the axle's steering gear ratio. The *At Axle* option allows different steer angles at the right-side and left-side wheels. The steer degree of freedom, describe earlier, my also be employed.

HVE Driver Model

SIMON supports the HVE Driver Model. The HVE Driver Model is a closed-loop driver control model that uses driver control attributes and the SIMON vehicle dynamics model to attempt to follow a user-specified path. This model is described in detail in reference 16.

Braking

Braking inputs may be provided for each wheel. The *At Pedal* option is the most robust model and its use is recommended. Using the *At Pedal* option causes SIMON to use the brake torque ratio supplied for each individual wheel. Wheel spin inertias and coupling within the differential are also included when the *At Pedal* option is selected. Resulting wheel torques are used in the wheel spin degree of freedom, described earlier. This model is capable of supporting a sophisticated ABS braking model. Such a model is under consideration.

Braking Force and *Percent Available Friction* brake table options are also allowed. If either of these methods is used, spin inertias and differential coupling are irrelevant and are ignored.

HVE Brake Designer

If the *At Pedal* braking option is selected, SIMON can use the HVE Brake Designer. Detailed brake component designs can be created and edited using the Brake Designer. The resulting brake design is then used during SIMON simulations. The brake torque is calculated dynamically for each wheel according to the mechanical design of the brake assembly as well as the current brake pressure, lining/drum temperature and sliding speed. The current lining friction is determined from the lining temperature and sliding speed, thus, brake fade can be simulated.

The HVE Brake Designer is described in detail in the HVE Designer Manual [6]. Additional information may be found in reference 15.

Throttle

Throttle inputs may be provided for each drive axle. *The Percent Wide-open Throttle* (*% WOT*) option is the most robust and its use is recommended. Using the *% WOT* option causes SIMON to use the HVE Drivetrain Model. Wheel spin inertias and coupling within the differential are also included when the *% WOT* option is selected.

Tractive Effort and *Percent Available Friction* options are also allowed. If either of these methods is used, spin inertias and differential coupling are irrelevant and are ignored.

Gear Selection

If the *% WOT* throttle option (above) is selected, the Gear Selection table is used for setting the time and gear selections for each gear shift.

If no gear selection entries are made, the vehicle's transmission will be in neutral and no amount of throttle will cause the vehicle to accelerate.

Wheel Position

Calculation of wheel center earth-fixed coordinates requires a transformation from the vehicle-fixed reference frame to the inertial reference frame. This transformation matrix, *A*, is given by

$$A = \begin{bmatrix} A_{11} & A_{12} & A_{13} \\ A_{21} & A_{22} & A_{23} \\ A_{31} & A_{32} & A_{33} \end{bmatrix} \qquad \text{(Eq. 19)}$$

where

$$\begin{aligned}
A_{11} &= \cos\psi\cos\phi \\
A_{12} &= \sin\psi\cos\theta \\
A_{13} &= -\sin\theta \\
A_{21} &= -\sin\psi\cos\phi + \cos\psi\sin\phi\sin\theta \\
A_{22} &= \cos\psi\cos\phi + \sin\phi\sin\psi\sin\theta \\
A_{23} &= \cos\theta \\
A_{31} &= \sin\psi\sin\phi + \cos\psi\sin\theta\cos\phi \\
A_{32} &= -\cos\psi\sin\phi + \sin\psi\sin\theta\cos\phi \\
A_{33} &= \cos\theta\cos\phi
\end{aligned}$$

and

ψ = Vehicle yaw angle
θ = Vehicle pitch angle
ϕ = Vehicle roll angle

(The order of rotations is *yaw, pitch, roll*.)

Calculation of these Euler angles requires integration of the rotational velocity components, *p,q,r*. Integration of these components along the axes of rotation of the Euler angles yields their angular velocity components,

$$\dot{\psi} = \left(q\sin\phi + r\cos\phi\right)\sec\theta \qquad \text{(Eq. 20)}$$

$$\dot{\theta} = q\cos\phi - r\sin\phi \qquad \text{(Eq. 21)}$$

$$\dot{\phi} = p + \left(q\sin\phi + r\cos\phi\right)\tan\theta \qquad \text{(Eq. 22)}$$

Note that the presence of $\tan\theta$ and $\sec\theta$ results in a singularity at 90 degree pitch angle. If necessary, an axis indexing scheme can be implemented to eliminate this singularity.

Given the current vehicle sprung mass orientation in space, the earth-fixed (inertial) wheel center coordinates are

$$\begin{bmatrix} X_w \\ Y_w \\ Z_w \end{bmatrix} = \begin{bmatrix} X_{CG} \\ Y_{CG} \\ Z_{CG} \end{bmatrix} + A \cdot \begin{bmatrix} x_w \\ y_w \\ z_w \end{bmatrix} \qquad \text{(Eq. 23)}$$

where

$\left[X_w Y_w Z_w\right]^T$ = Earth-fixed wheel center coords

$\left[X_{CG} \quad Y_{CG} \quad Z_{CG}\right]^T$ = Earth-fixed vehicle CG coordinates

$\left[x_w y_w z_w\right]^T$ = Vehicle-fixed wheel center coordinates

The calculation of vehicle-fixed wheel center coordinates is dependent upon the suspension type.

Vehicle-fixed Wheel Orientation

Wheel orientation with respect to the vehicle-fixed coordinate system is defined by three angles (see Figure 8):

Wheel Steer, δ_w - Wheel rotation about an axis parallel to the vehicle-fixed z (yaw) axis

Wheel Camber, γ_w - Wheel rotation about an axis parallel to the vehicle-fixed x (roll) axis

Wheel Spin, ω_w - Wheel rotation about an axis parallel to the vehicle-fixed y (pitch) axis.

Wheel spin is calculated by the equations of motion for each wheel (see Eqs. 8 through 13). If the steer degree of freedom option is selected, wheel steer is calculated by the

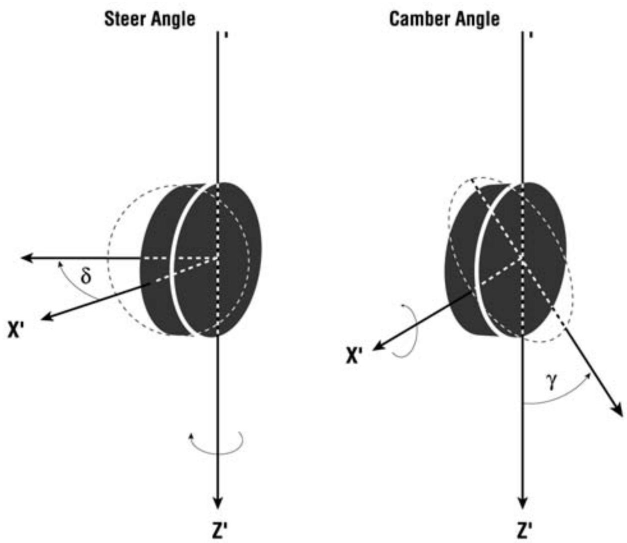

Figure 8 - Vehicle-fixed wheel orientation.

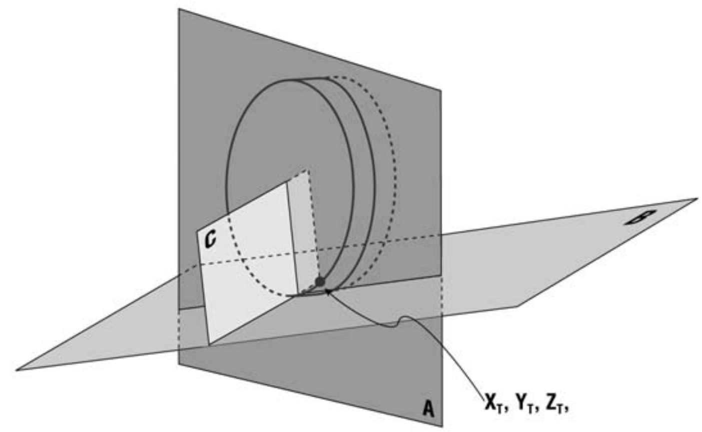

Figure 9 - Wheel-terrain geometry.

equations of motion for the steering system (see Eqs. 14 and 15). Otherwise, wheel steer and wheel camber are determined from user-defined suspension properties, look-up tables and driver control tables. The manner in which the wheel orientations are calculated is dependent upon suspension type. The details of this development are presented in reference 14.

Tire Contact Patch Velocity

The calculation of tire forces requires definition of the tire slip angle, which, in turn, requires calculation of velocity components at the tire contact patch. These velocity components are first calculated in the vehicle-fixed reference frame and then projected onto the ground plane beneath the tire. The calculation of these velocity components is a function of the vehicle's current CG velocity, vehicle-fixed wheel position and suspension type. The details of this development are presented in reference 14.

Tire-Road Contact Patch

Tire force calculations require that the tire-road interface be defined in terms of normal and shear forces, and resulting tire deflection. To perform these calculations requires a careful analysis of the wheel's orientation with respect to an arbitrary surface (terrain). As shown in Figure 9, this point is the intersection of three planes: Plane *A* is the tire plane, plane *B* is the terrain beneath the tire and Plane *C* is a plane perpendicular to planes *A* and *B* and passing through the wheel center.

Terrain Definition

The first step is to define the terrain (contact patch coordinates, friction multiplier and surface normal) beneath the tire.SIMON performs this step by calling HVE's `GetSurfaceInfo()` function. Given the current earth-fixed coordinates, $X_t, Y_t,$ of the tire's center of rotation, `GetSurfaceInfo()` searches the entire environment polygon database until it finds the polygon beneath the tire (see Figure 10). For this polygon, `GetSurfaceInfo()` returns the earth-fixed elevation, Z_t, beneath the tire center, as well as the friction multiplier, *f*, and unit vector, $\vec{U}_{Terrain}$, representing the surface normal for the polygon directly beneath each tire.

Tire-Ground Orientation

The tire-ground orientation is defined by the tire inclination angle, γ_w, and steer angle, δ_w, relative to the surface beneath the wheel, as shown in Figure 8. A line in the earth-fixed coordinate system normal to the wheel plane is defined by a unit vector, $\vec{U}_w$,

$$\vec{U}_w = \begin{bmatrix} u_{w_X} \\ u_{w_Y} \\ u_{w_Z} \end{bmatrix} = A \cdot \begin{bmatrix} -\sin\delta_w \\ \cos\gamma_w \cos\delta_w \\ \sin\gamma_w \cos\delta_w \end{bmatrix} \qquad \text{(Eq. 24)}$$

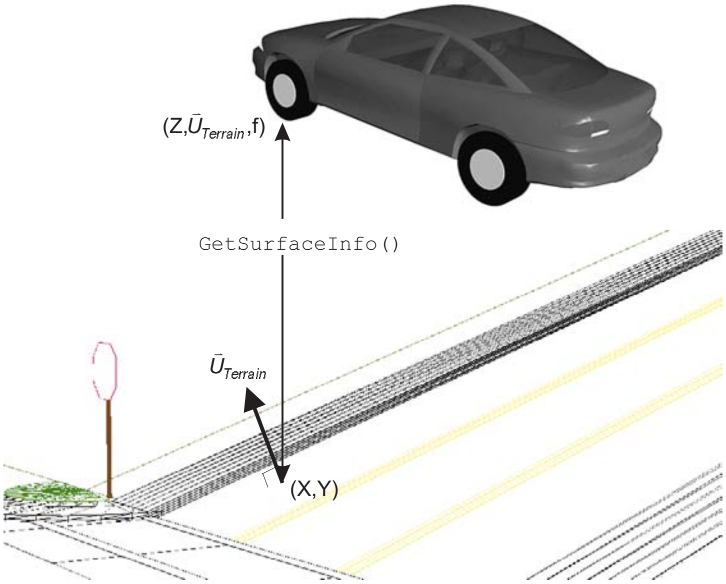

Figure 10 - GetSurfaceInfo() returns the terrain surface elevation, Z, friction multiplier, f, and surface normal, $\bar{U}_{Terrain}$, for the earth-fixed X,Y coordinates beneath the tire.

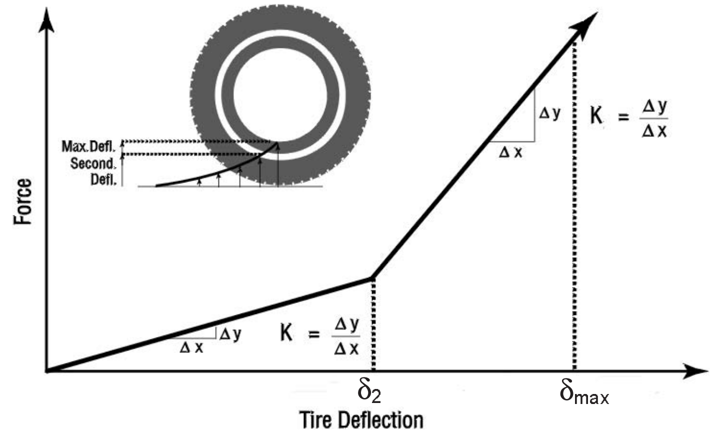

Figure 11 - 2-step radial tire stiffness used for calculating the current tire radial force.

where

A = Transformation matrix (see Eq. 19)

γ_w = Vehicle-fixed camber angle

δ_w = Vehicle-fixed steer angle

Tire Radial Deflection

Once the contact point is determined, the tire radial deflection can be calculated directly from the earth-fixed distance, D, between the wheel center, X_w, Y_w, Z_w, and the tire-ground contact point, X_T, Y_T, Z_T

$$D = \sqrt{\left(X_w - X_T\right)^2 + \left(Y_w - Y_T\right)^2 + \left(Z_w - Z_T\right)^2}$$

(Eq. 25)

Based on the distance from the wheel center to the terrain contact point, the current tire rolling radius, r, is

$$r = \begin{cases} D, & \text{for } D < r_u \\ r_u, & \text{for } D \geq r_u \end{cases} \quad \text{(Eq. 26)}$$

where r_u is the unloaded radius.

It is now a simple matter to calculate the tire radial deflection, δ_T, in the wheel plane by comparing the tire unloaded radius with the current tire radius,

$$\delta_T = r_u - r \quad \text{(Eq. 27)}$$

Tire Radial Force

Tire radial force is calculated in the direction of the tire deflection according to the tire force-deflection properties (see Figure 11) and current deflection,

$$F_R = \begin{Bmatrix} \xi K_T \delta_T, \ \text{for } \delta_T < \delta_2 \\ \xi K_T \left(K_{T_2}\left(\delta_T - \delta_2\right) + \delta_2\right), \ \text{for } \delta_T \geq \delta_2 \end{Bmatrix}$$

(Eq. 28)

where

F_R = Radial tire force (force in the tire plane in the direction of the tire deflection)

K_T = Tire initial radial stiffness

K_{T_2} = Tire secondary stiffness multiplier

δ_2 = Tire radial deflection at which K_{T_2} begins (tire radial force, continued):

ξ = Tire restitution characteristic

$$= \begin{Bmatrix} 1.0, & \text{for } \delta_r > \delta_{r_{previous\ timestep}} \\ \lambda, & \text{for } \delta_r \le \delta_{r_{previous\ timestep}} \end{Bmatrix}$$

λ = Tire stiffness multiplier ($0 \le \lambda \le 1$) for rebound

Tire radial force, F_R, is an important fundamental property as one of the primary inputs to the tire model that is used to calculate tire braking and cornering force.

Tire Model

SIMON uses the EDC semi-empirical tire model developed for EDVDS [9,10]. The basis for the EDC semi-empirical tire model is the HSRI tire model, developed at the University of Michigan Transportation Research Institute [23]. The model was extended to allow large tire slip angles, drive torque (i.e., tire forces that accelerate the vehicle) and drive and/or brake torque when the vehicle is rolling backwards. The SIMON implementation for load- and speed-dependent tire properties has been extended by replacing the method of partial derivatives with a table look-up method. An overview of the extended model is provided in reference 14 for purposes of comparison with the HSRI and EDVDS tire models.

Rolling Resistance

The original EDC semi-empirical tire model has also been extended to include a circumferential tire moment from rolling resistance. The rolling resistance moment, $M_{Rolling}$, is given by

$$M_{Rolling} = r\left(\sigma_0 F_R + \sigma_v \left|u_{GP}\right|\right) \cdot sign(\Omega) \qquad \text{(Eq. 29)}$$

where

r = Tire rolling radius

σ_0 = Load-dependent rolling resistance coefficient

σ_v = Velocity-dependent rolling resistance coefficient

F_R = Radial tire force

u_{GP} = Vehicle-fixed forward component of tire velocity in the ground plane

Ω = Wheel spin angular velocity

The rolling resistance moment contributes to the equations of motion for the wheel spin degree of freedom (see Eqs. 8 through 13).

Suspension Force

Independent and solid axle suspensions are supported in SIMON. The equations of motion for each suspension type are discussed in reference 14 (see Eqs. 7 through 10 and 18 through 26). Suspension force calculations for both models are identical. The force is calculated using a spring-damper model with additional coulomb friction, as shown in the model in Figure 12. The spring is free to move only in the vehicle-fixed z-direction. The total suspension force is the sum of the spring force, damping (shock absorber) force and coulomb friction force. The force from an anti-sway bar, used for producing additional roll stiffness, is also included in the model. Mathematically, the force, F_s, at each suspension location is

$$F_S = K\delta + C\dot{\delta} + F_\mu + \frac{K_{rs}}{\vec{r}_s}\phi_{Axle} \qquad \text{(Eq. 30)}$$

where

K = Linear spring rate of suspension spring

δ = Spring deflection from equilibrium (+ down)

C = Velocity-dependent damping rate

$\dot{\delta}$ = Spring deflection rate

F_μ = Coulomb friction force

K_{rs} = Auxiliary roll stiffness of anti-sway bar

$\vec{r}_s$ = Spring location, y-coordinate

ϕ_{Axle} = Vehicle-fixed axle roll angle

The model also includes suspension stops for both jounce (-) and rebound (+) spring deflections (see Figure 13). The effect of a suspension stop is to limit suspension travel by increasing significantly the suspension stiffness. The suspension force generated at a suspension stop is expressed mathematically as

$$F_{Stop} = \begin{Bmatrix} K_1\delta_{Stop} + K_3\delta_{Stop}^3, & \text{for } \delta \cdot \dot{\delta} \ge 0 \\ \eta\left(K_1\delta_{Stop} + K_3\delta_{Stop}^3\right), & \text{for } \delta \cdot \dot{\delta} < 0 \end{Bmatrix}$$

(Eq. 31)

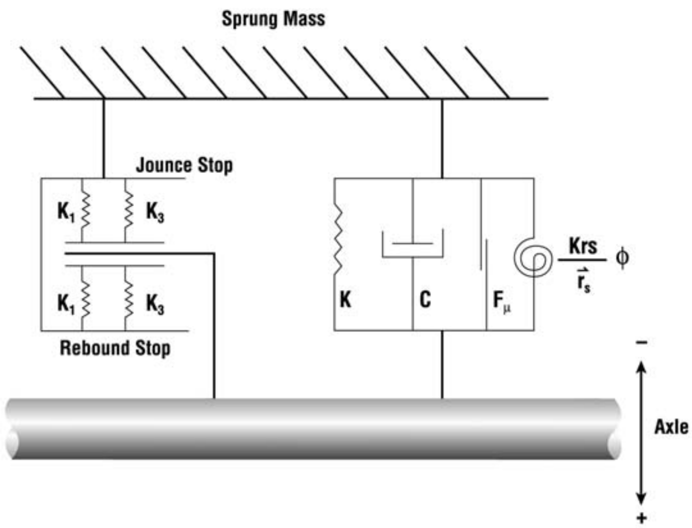

Figure 12 - Suspension force model.

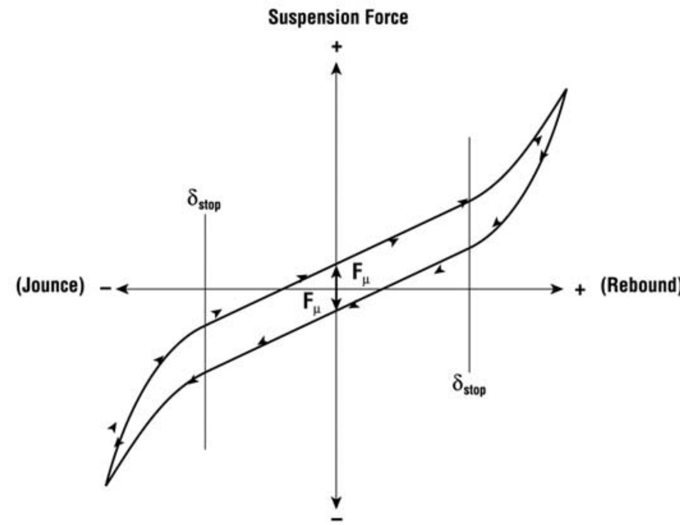

Figure 13 - Force produced by suspension stops.

where

K_1	= Stop linear rate
K_3	= Stop cubic rate
δ_{Stop}	= Deformation of suspension stop
η	= Stop energy ratio (a restitution coefficient)
$\delta \cdot \dot{\delta}$	= (-) if stop deformation is decreasing (used for reducing F_{Stop}; see Eq. 31)

Inter-Vehicle Connection Model

In a multi-vehicle train (e.g., a tractor-semitrailer), each sprung mass is allowed six degrees of freedom. The sprung masses are connected by constraint forces and moments acting at the inter-vehicle connection points, as shown in Figure 14.

Connection Force

The constraint force is first calculated in the inertial (earth-fixed) reference system, then resolved according to each vehicle-fixed system. In the earth-fixed system,

$$\vec{F}_C = \left(\vec{R}_n - \vec{R}_{n+1}\right) \cdot K_C + \left(\vec{V}_n - \vec{V}_{n+1}\right) \cdot C_C \quad \text{(Eq. 32)}$$

where

$\left\Vert \vec{R}_n - \vec{R}_{n+1} \right\Vert$	=	Earth-fixed distance between connection points on vehicles *n* and *n+1*
K_C	=	Constraint spring rate for vehicle pair
	=	$\min\left(mass_{n_{Sprung}}, mass_{n+1_{Sprung}}\right) \cdot g$
$\left\Vert \vec{V}_n - \vec{V}_{n+1} \right\Vert$	=	Earth-fixed relative speed between connection points on vehicles *n* and *n+1*
C_C	=	Constraint damping rate for vehicles *n* and *n+1*
	=	$0.5\sqrt{K_{C_n} \min\left(mass_{n_{Sprung}}, mass_{n+1_{Sprung}}\right)}$

Connection Moments

SIMON models roll and yaw moment transfers between connected vehicles. The roll moment is the result of a difference in roll angle between connected vehicles and the yaw moment results from friction in the connection.

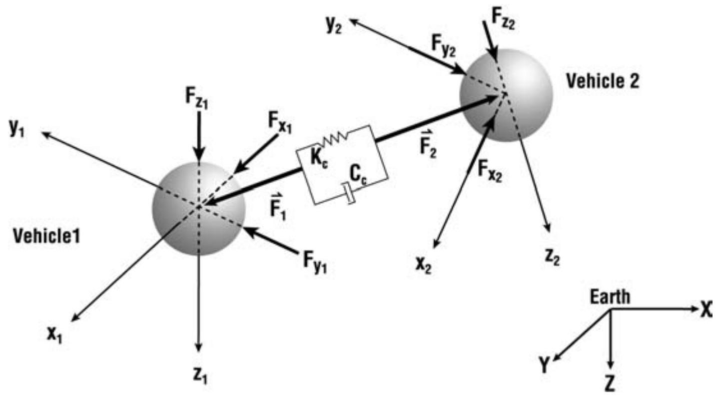

Figure 14 - Inter-vehicle connection force.

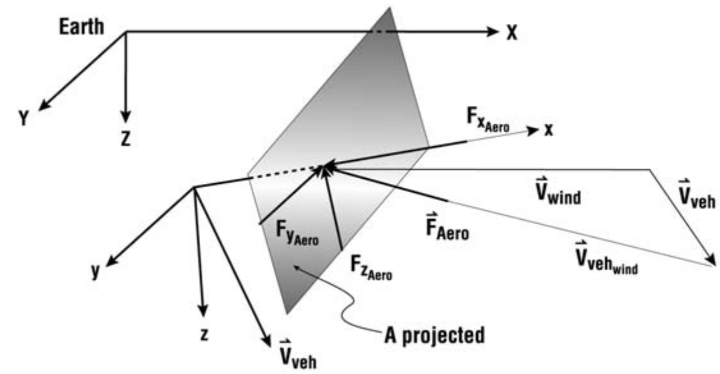

Figure 16 - Aerodynamic forces and moments.

Dollys

Two types of dollys are supported by SIMON (see Figure 15):

Converter Dolly - The fifth wheel articulates about the pitch axis, and the drawbar is rigidly attached to the dolly. The result is that brake torque is resisted at the pintle hook of the tow vehicle. Thus, trailer braking results in a vertical load transfer to the rear of the tow vehicle.

Fixed Dolly - The fifth wheel is fixed to the trailer and is not free to articulate about its pitch axis. The drawbar is hinged. Thus, there is no load transfer to the tow vehicle.

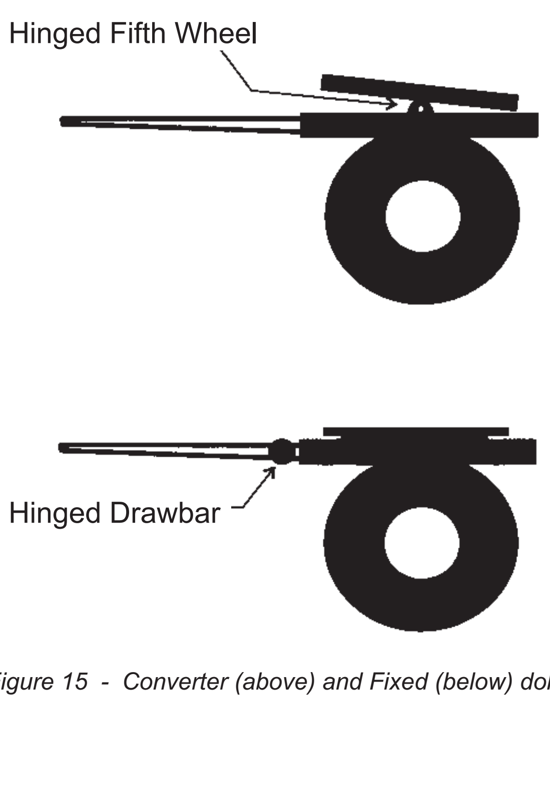

Figure 15 - Converter (above) and Fixed (below) dollys.

Aerodynamics Model

SIMON includes a lump parameter aerodynamics model that includes drag on all six vehicle surfaces (front, back, right, left, top and bottom), as well as two additional, user-defined devices, such as a front or rear wing (see Figure 16). Air properties (temperature and pressure) are supplied by the Environment Editor, allowing SIMON to study various effects, such as cross-wind, on vehicle handling performance.

Aerodynamic forces and moments produced by each surface act on the sprung mass. To compute these forces, the earth-fixed wind velocity must first be calculated,

$$\vec{V}_{Wind} = \begin{bmatrix} V_{X_{Wind}} \\ V_{Y_{Wind}} \\ V_{Z_{Wind}} \end{bmatrix} = \begin{bmatrix} S_{Wind} \cos(\psi_{Wind} - \pi) \\ S_{Wind} \sin(\psi_{Wind} - \pi) \\ 0 \end{bmatrix} \qquad \text{(Eq. 33)}$$

where

S_{Wind} = User-entered wind speed

ψ_{Wind} = User-entered wind direction relative to earth-fixed X-axis

Sprung Mass Impact Model

SIMON uses HVE's DyMESH collision model [18,19] to compute 3-dimensional forces and moments resulting from inter-vehicle collision. Simultaneous collision forces between any number of vehicles are allowed.

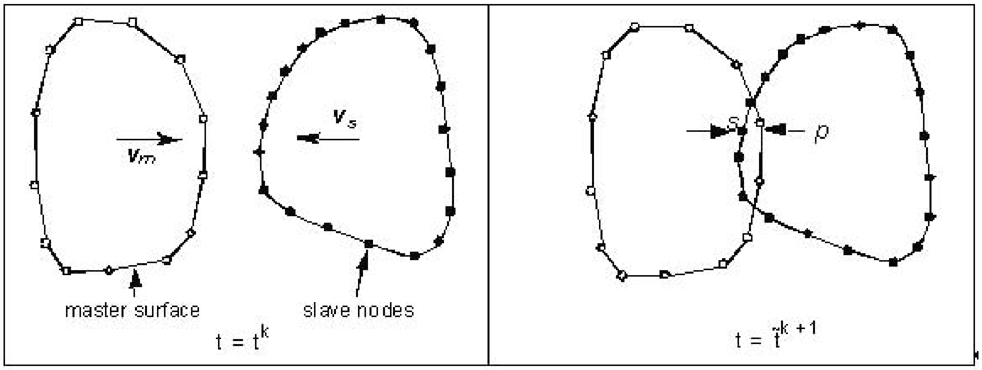

Figure 17 - DyMESH Master Surface - Slave Node concept.

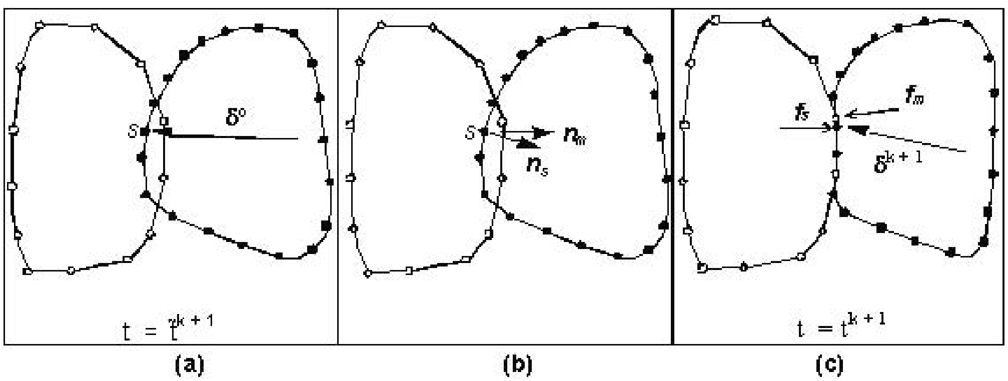

Figure 18 - DyMESH Restoration phase.

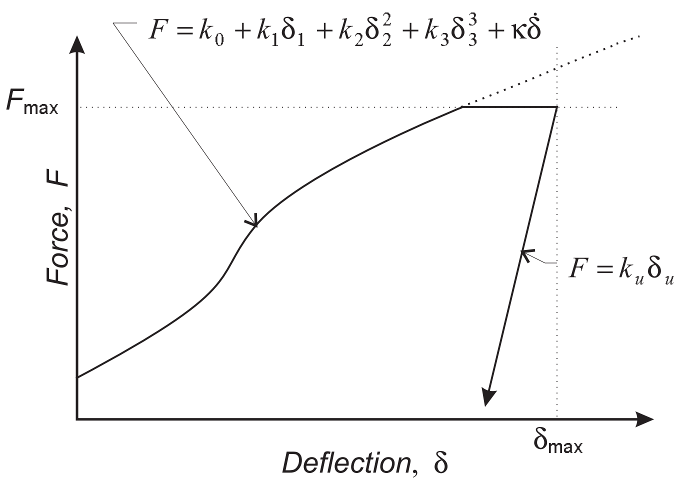

Figure 19 - Force-deflection relationship used in DyMESH.

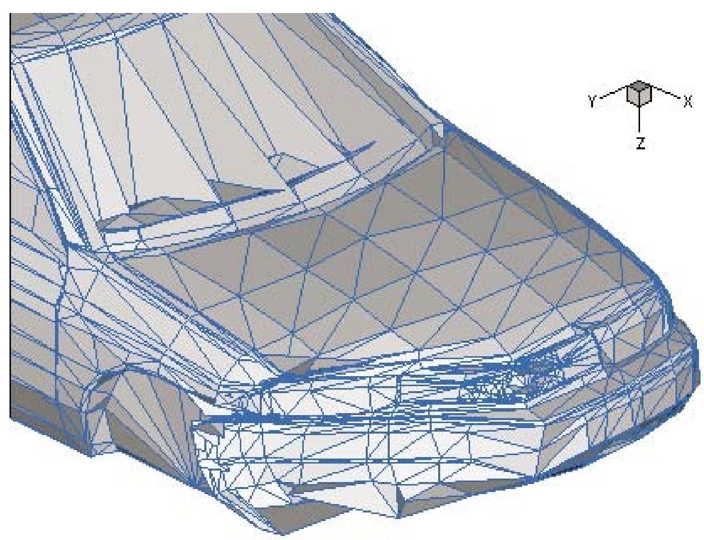

Figure 20 - DyMESH example.

The DyMESH method is based on a collision algorithm which uses a triangular mesh defined by descretizing the vehicle exterior surface(s). The algorithm detects the interaction between vehicles by monitoring the positions of nodes, or vertices, and surface polygons representing the vehicle exterior. The concept of a master surface and a slave node is used. This mirrors proven technology used with contact algorithms for many years.

The basic operations in the contact algorithm are *location* and *restoration*. Location involves searching for surfaces in contact with one another and defining contact geometry, such as depth of penetration of the node of one vehicle into the surface polygons of another. Restoration involves finding the penetration depth of the (slave) node and moving it back to the (master) surface.

Figure 17 shows two generalized body meshes descretized on their exterior with surface and node elements. Consider the left body to be the master and the right body to be the slave. At time t, the bodies are moving towards each other with velocities V_m and V_s, but there is no contact. At time $t+\Delta t$, several slave nodes have penetrated the master surfaces. For example, node S has penetrated a distance p.

Once penetration is detected, the pushback direction is determined and slave node S is restored to its contact point on the master surface (see Figure 18).

After the slave node is restored, as shown in Figure 18c, the vector δ^{k+1} is calculated. The force on the slave node is a function of the vehicle node stiffness parameters, the volume of the material associated with the crush of slave node S, and $\Delta\delta$, where

$$\Delta\delta = \left|\delta^0 - \delta^{k+1}\right| \qquad \text{(Eq. 34)}$$

During loading, the collision force on each node is based on a general purpose, 3rd-order polynomial force-deflection relationship supplied by the user of the form

$$F_{node} = k_0 + k_1\Delta\delta + k_2\Delta\delta^2 + k_3\Delta\delta^3 + \kappa\left(\Delta\dot{\delta}\right) \qquad \text{(Eq. 35)}$$

where

k_n = 3rd-order polynomial coefficients

$\Delta\delta$ = Node penetration distance

κ = Velocity-dependent damping coefficient

The force-deflection relationship may also include a saturation force, F_{max}, and a saturation deflection, δ_{max}. See Figure 19.

During unloading, the collision force is determined by an unloading slope, K_u. Specification of the unloading slope allows the model to account for restitution. The presence of unloading is determined by the deformation rate.

The DyMESH collision model is described in references 7 and 8. In general, vehicle-fixed deformation (see Figure 20) and force components are calculated for each vertex. These forces are summed and the resulting summed forces and moments acting on the sprung mass are supplied to the dynamics engine (see Eq. 3).

SOFTWARE IMPLEMENTATION

The SIMON physics model and component modules are implemented in a single HVE-compatible physics program. All HVE-compatible physics programs are executed as a child process within the HVE Simulation Environment. As shown in Figure 21, the HVE Simulation Environment provides editors for creating and editing humans, vehicles and environments, as well as an editor for setting up and executing events (an event is an individual execution of a physics model, such as SIMON, with the selected human(s), vehicle(s) and environment) and an editor for displaying reports and creating videos.

SIMON is programmed using the C programming language. It is a modular program and includes several C functions to perform specific tasks. A general flow chart for SIMON is shown in Figure 22.

DISCUSSION

The validation of SIMON is under way. The validation compares SIMON results with actual test results from handling and collision experiments conducted at the Exponent Failure Analysis Associates Test and Engineering Center. Preliminary results reveal reasonable correlation between simulation and experimental results. A complete validation study will be made available soon.

Close inspection of the SIMON model reveals it is very general and more powerful than previous simulations. For example, each wheel location is specified individually (e.g., front wheels are not constrained to lie the same distance ahead of the vehicle CG, nor are they constrained to lie the same distance laterally from the CG). This generality in the model allows SIMON to simulate interesting effects, such as wheels that are displaced during a collision. This generality also allows SIMON to include the effect of occupant loading on vehicle weight distribution. Although heavy (or multiple) occupants can clearly affect vehicle handling behavior, no previous simulation has been found that includes the ability to study this behavior.

The system-based design approach employed by SIMON allows multiple design teams to work together using the same basic model. For example, the chassis group

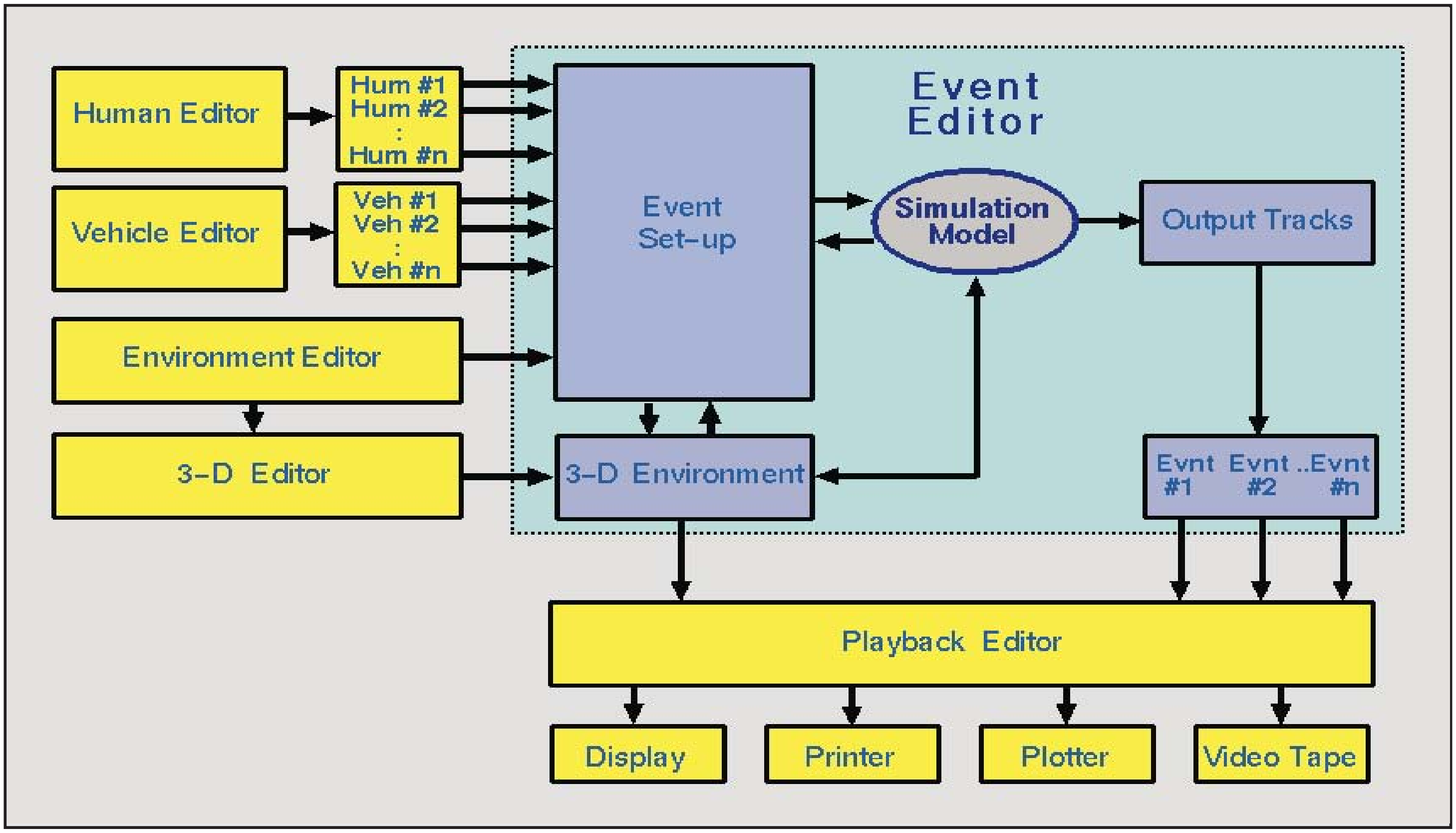

Figure 21 - HVE Simulation Environment [1].

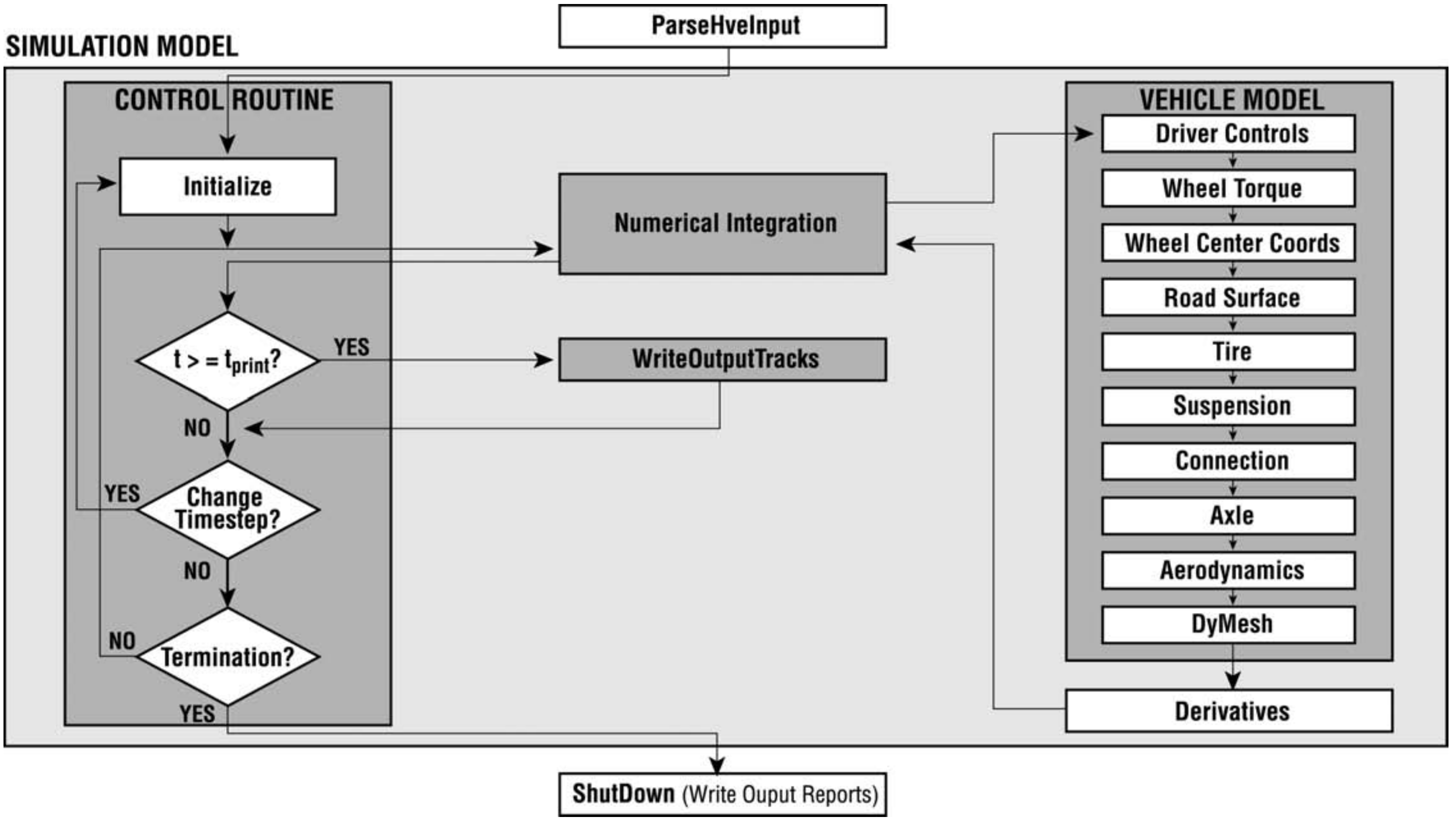

Figure 22 - Flowchart for SIMON main calculation procedures.

can use the HVE Drivetrain Model that includes detailed descriptions for the engine, transmission and differential. The HVE Brake Designer allows SIMON to be used for detailed design of brake system components for all types of disc and drum brakes. The model also allows failure analysts to better understand brake system component failure mechanisms (e.g., the effect of brake adjustment on shoe and drum temperature). The use of virtual accelerometers allows safety researchers to study occupant speed changes at various seat locations within the vehicle. The aerodynamics model employed by SIMON is a significant improvement over previous models. The EDC Semi-empirical Tire Model employed by SIMON, originally developed for the EDVDS model [9,10], has been extended by the use of load- and speed-dependent table look-up methods. Wheel steer and spin degrees of freedom represent further improvements over previous models, providing the basis for the HVE Driver Model and the detailed analysis of drive and brake torque at the tire-road interface.

The use of DyMESH, a truly 3-dimensional time-domain collision simulation model, is also new to a general purpose vehicle handling simulation. This capability will allow crash researchers to simulate collisions involving bumper over-ride and to simulate with greatly improved fidelity post-crash rollover initiated by collision-related roll and pitch moments. Multi-vehicle and articulated vehicle collisions are handled inherently.

A key design goal for SIMON was that it be a single tool that is useful to the entire spectrum of users, throughout the vehicle life cycle - from initial design to post-crash analysis. For example, the vehicle model includes enough detail to be useful to vehicle engineers working with issues such as suspension design and tire selection. The environment model allows test engineers to develop digital proving grounds and perform proof-of-concept simulations on the computer before investing in the development and testing of expensive prototype designs. Human, vehicle and tire databases and 3-dimensional environment modeling also allow the routine use of SIMON in crash reconstructions. The authors feel the use of one tool by all these fields can improve communication between these fields and, therefore, improve the overall vehicle design process.

CONCLUSIONS and RECOMMENDATIONS

The SIMON vehicle simulation has been described. SIMON's basic feature set and modeling equations have been presented in detail. SIMON provides a robust modeling method for design engineers and safety researchers needing the model vehicle dynamic behavior.

A validation study is required. The validation study currently under way will determine the fidelity of SIMON for several different types of applications, including handling (both simple and limit maneuvers), combination vehicle and trailer train dynamic simulation, 3-dimensional collision simulation and rollover events.

The implementation of SIMON as an HVE-compatible simulation model provides a powerful, yet user-friendly environment for setting up and executing SIMON simulations and providing numeric, graphic and video reports.

REFERENCES

1. Day, T.D., "A Computer Graphics Interface Specification for Studying Humans, Vehicles and their Environment," SAE Paper No. 930903, Society of Automotive Engineers, Warrendale, PA, 1993.

2. Day, T.D., "An Overview of the HVE Developer's Toolkit," SAE Paper No. 940923, Society of Automotive Engineers, Warrendale, PA, 1994.

3. Day, T.D., "An Overview of the HVE Vehicle Model," SAE Paper No. 950308, Society of Automotive Engineers, Warrendale, PA, 1995.

4. Day, T.D., "An Overview of the HVE Human Model," SAE Paper No. 950659, Society of Automotive Engineers, Warrendale, PA, 1995.

5. Day, T.D., "Validation of Several Reconstruction and Simulation Models in the HVE Scientific Visualization Environment," SAE Paper No. 960891, Society of Automotive Engineers, Warrendale, PA, 1996.

6. *HVE User's Manual,* Third Edition, Engineering Dynamics Corporation, Beaverton, OR, 2000.

7. Day, T.D., "Validation of the EDVSM 3-Dimensional Vehicle Simulator," SAE Paper No. 970958, Society of Automotive Engineers, Warrendale, PA, 1997.

8. *EDVSM User's Manual,* Third Edition, Engineering Dynamics Corporation, Beaverton, OR, 2000.

9. Day, T.D., "Differences Between EDVDS and Phase4," SAE Paper No. 1999-01-0102, Society of Automotive Engineers, Warrendale, PA, 1999.

10. *EDVDS User's Manual,* Third Edition, Engineering Dynamics Corporation, Beaverton, OR, 2000.

11. *EDHIS User's Manual*, Third Edition, Engineering Dynamics Corporation, Beaverton, OR, 2000.

12. Day, T.D., "An Overview of the EDSMAC4 Collision Simulation Model," SAE Paper No. 1999-01-0102, Society of Automotive Engineers, Warrendale, PA, 1999.

13. *EDSMAC4 User's Manual,* Third Edition, Engineering Dynamics Corporation, Beaverton, OR, 2000.

14. *SIMON User's Manual,* First Edition, Engineering Dynamics Corporation, Beaverton, OR, 2000.

15. Roberts, S.G., Day, T.D., "Integrating Design and Virtual Test Environments for Brake Component Design and Material Selection," SAE Paper No. 2000-01-1294, Society of Automotive Engineers, Warrendale, PA, 2000.

16. Day, T.D., Metz, L.D., "The Simulation of Driver Inputs Using a Vehicle Driver Model," SAE Paper No. 2000-01-1313, Society of Automotive Engineers, Warrendale, PA, 2000.

17. Blythe, W., Day, T.D., Grimes, W.D., "3-Dimensional Simulation of Vehicle Response to Tire Blow-outs," SAE Paper No. 980221, Society of Automotive Engineers, Warrendale, PA, 1998.

18. York, A.R., Day, T.D., "The DyMESH Method for Three-Dimensional Multi-Vehicle Collision Simulation," SAE Paper No. 1999-01-0104, Society of Automotive Engineers, Warrendale, PA, 1999.

19. Day, T.D., York, A.R., "Validation of DyMESH for Vehicle vs. Barrier Collisions," SAE Paper No. 2000-01-0844, Society of Automotive Engineers, Warrendale, PA, 2000.

20. Canova, J.H., "Vehicle Design Evaluation Using the Digital Proving Ground," SAE Paper No. 2000-01-0126, Society of Automotive Engineers, Warrendale, PA, 2000.

21. *Vehicle Dynamics Terminology,* SAE Recommended Practice J-670e, Society of Automotive Engineers, Warrendale PA., 1976.

22. Etkin, B., *The Dynamics of Flight, Stability and Control*, 3rd Edition, John Wiley and Sons, New York, NY, 1995.

23. MacAdam, C.C., Fancher, P.S., Hu, G.T., Gillespie, T.D., "A Computerized Model for Simulating the Braking and Steering Dynamics of Trucks, Tractor-Semitrailers, Doubles and Triples Combination - User's Manual," Highway Safety Research Institute, University of Michigan Report No. UM-HSRI-80-58, Final Report, 1980.

Reviewer's Discussion
by Dennis P. Martin, PE, MDE Engineers, Inc., Seattle

SAE #2001-01-0503
"SIMON: A New Vehicle Simulation Model for Vehicle Design and Safety Research",
Authors, Terry D. Day and Sydney G. Roberts, Engineering Dynamics Corporation, and Allen R. York, York Engineering

This paper presents the basic technical foundation for the new simulation model. The presentation is clear and concise and provides a valuable reference tool in the field of simulation of vehicle dynamics and collisions. We await the validation studies to assess the accuracy and utility of the model. This reviewer made no attempt to check the accuracy of the various analytical methods presented. The new model is broad in its scope in that it covers the capabilities of other models that preceded it and also greatly expands the capabilities of the prior art. The model is particularly impressive in that the user can vary such inputs as the steering column rotational inertia and friction and the user can precisely position the mass of the occupants and cargo. These are but a few of the expanded capabilities of the model. The paper should also be of use to researchers who may be contemplating developing or modifying similar models.